

REVIEW



CrossMark  
click for updates

Cite this: *J. Mater. Chem. A*, 2016, 4, 5773

Received 30th December 2015  
Accepted 9th March 2016

DOI: 10.1039/c5ta10737g

www.rsc.org/MaterialsA

## CeO<sub>2</sub>-based heterogeneous catalysts toward catalytic conversion of CO<sub>2</sub>

Fei Wang, Min Wei,\* David G. Evans and Xue Duan

The catalytic conversion of CO<sub>2</sub>, which has recently attracted considerable attention, would not only contribute to the alleviation of environmental problems but would also provide useful chemicals (e.g., methane and methanol). Due to the thermodynamic stability of CO<sub>2</sub>, developing highly efficient and cost-effective catalysts is the main challenge with respect to large scale production. CeO<sub>2</sub>-based materials have aroused increasing research interest as supports or catalysts toward CO<sub>2</sub> conversion. By virtue of the unique structural properties resulting from oxygen vacancies and reversible valence change (Ce<sup>4+</sup> and Ce<sup>3+</sup>), CeO<sub>2</sub> exhibits great potential as a support to immobilize catalytically-active species or even as an active site to activate the oxygen-containing bond in catalytic reactions involving CO<sub>2</sub>. In this review, the latest advances in the design, preparation and application of CeO<sub>2</sub>-based heterogeneous catalysts toward CO<sub>2</sub> conversion are summarized.

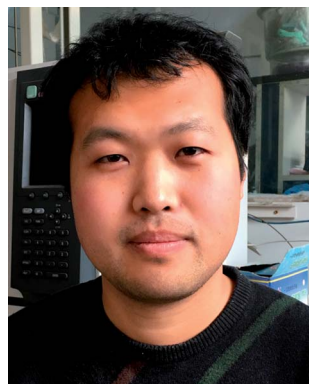
### 1. Introduction

In recent decades, global warming caused by the increasing CO<sub>2</sub> concentration in the atmosphere (mainly produced by the burning of fossil fuels) has attracted considerable attention.<sup>1,2</sup> As a safe and abundant carbon source, the utilization of CO<sub>2</sub> to achieve carbon recycling not only contributes to the alleviation of environmental problems but also has the potential to provide useful chemicals (e.g., methane and methanol).<sup>3,4</sup> A great many scientific breakthroughs on this meaningful topic have been

achieved from a wide scope of research fields, including materials science, catalysis, photocatalysis and sustainable chemistry.<sup>5-7</sup> Among these, CO<sub>2</sub> conversion promoted by heterogeneous catalysis has aroused intense interest due to its economic efficiency and industrial application. However, the effective transformation of CO<sub>2</sub> still raises challenges due to the difficulties in activating the thermodynamically stable CO<sub>2</sub>, which requires high temperatures with an energy-intensive process.<sup>8,9</sup> For this reason, the rational design and preparation of efficient heterogeneous catalysts with high performance and stability are of vital importance in realizing CO<sub>2</sub> conversion on a large scale.

CeO<sub>2</sub>, as a well-studied heterogeneous catalyst or support, has attracted extensive research interest in a wide scope of reactions,

State Key Laboratory of Chemical Resource Engineering, Beijing University of Chemical Technology, Beijing 100029, China. E-mail: weimin@mail.buct.edu.cn; Fax: +86-10-64425385; Tel: +86-10-64412131



Fei Wang received his BS degree in 2009 from the Beijing University of Chemical Technology (BUCT). He joined Professor Xue Duan's group as a PhD candidate at BUCT in 2010, and he currently works on designing new catalysts toward CO<sub>2</sub> conversion.



Min Wei obtained her BS degree in 1995 and MS degree in 1998 from the Beijing University of Chemical Technology (BUCT). She subsequently received her PhD from the Peking University in 2001, after which she joined the staff of BUCT. She was promoted to full Professor in 2005. She has been a visiting scholar in the Georgia Institute of Technology (in 2008). Her research interests focus on inorganic-organic composite functional materials as well as new catalysts.

due to its unique structural properties resulting from oxygen vacancies and reversible valence change ( $\text{Ce}^{4+}$  and  $\text{Ce}^{3+}$ ).<sup>10–12</sup> In particular,  $\text{CeO}_2$ -based materials are appropriate catalysts toward  $\text{CO}_2$  conversion (such as photocatalytic<sup>13–15</sup> and heterogeneous catalytic reactions<sup>16–20</sup>) by virtue of these attractive structural features. The oxygen vacancies in  $\text{CeO}_2$  improve the activity and stability of supported metal nanoparticles;<sup>16–18</sup> moreover, they serve as active sites to activate the oxygen-containing bond in catalytic reactions involving  $\text{CO}_2$ .<sup>19,20</sup> In addition, the  $\text{Ce}^{3+}$  species as a Lewis base is beneficial to the adsorption and conversion of  $\text{CO}_2$ .<sup>21</sup> For instance, it can effectively promote the disproportionation of  $\text{CO}_2$  and the stabilization of CO-containing intermediates. However, the detailed roles of  $\text{CeO}_2$ -based materials in a specific reaction are normally very complicated, therefore need to be carefully studied in order to facilitate the development of novel catalysts.

In this *Overview Article*, we comprehensively summarize recent progress in the design and preparation of  $\text{CeO}_2$ -based catalysts towards  $\text{CO}_2$  conversion reactions (reverse water gas shift reaction,  $\text{CO}_2$  methanation, methanol synthesis from  $\text{CO}_2$  and  $\text{CO}_2$  reforming of methane). The catalytic role of  $\text{CeO}_2$  (as a support or a catalytic active site) in these reactions is reviewed based on preparation, characterization and structure-property correlation. In the final section, current challenges and future strategies are discussed from the viewpoint of intrinsic active sites and reaction mechanisms over a multi-step and structure-sensitive catalytic system. It is anticipated that this *Overview Article* will attract more attention toward  $\text{CeO}_2$ -based materials in the catalytic conversion of  $\text{CO}_2$  and encourage future work in this exciting and fast-growing area.

## 2. Reverse water gas shift (RWGS) reaction

The catalytic conversion of  $\text{CO}_2$  via the RWGS reaction is an important route to modify the  $\text{H}_2/\text{CO}$  ratio in syngas, which is then used for the synthesis of hydrocarbons.<sup>22–24</sup> Moreover, the

RWGS reaction is the reverse reaction of the WGS reaction, which plays an important role in industry. Studying the mechanism of the RWGS reaction is also instructive for understanding the WGS reaction and for the improvement of industrial catalysts.<sup>25</sup> For this reason, research on the RWGS reaction is valuable both in fundamental study and technological application.



The reaction mechanisms of the RWGS reaction are mainly classified into two categories. One is the redox mechanism:<sup>26</sup> hydrogen acts as a reducing reagent and does not participate in the formation of intermediates. The other mechanism involves formate as the intermediate, which comes from the adsorption and hydrogenation of  $\text{CO}_2$ ;<sup>27</sup> the CO is ultimately formed as the decomposition product of formate. Various types of catalyst have been developed for the RWGS reaction and of these,  $\text{CeO}_2$ -based material exhibited superior catalytic activity (Table 1).

### $\text{CeO}_2$ as support

$\text{CeO}_2$  is widely used as a support for heterogeneous catalysts due to its excellent performance in maintaining smaller particles of supported metal compared with other supports.<sup>16–18</sup> According to previous reports, metal nanoparticles tend to nucleate at oxygen vacancies and vacancy clusters on a  $\text{CeO}_{2-x}$  surface and bind more strongly to vacancy sites than to stoichiometric sites.<sup>36</sup> However, the detailed structure and evolution regularity of the  $\text{CeO}_{2-x}$  surface, especially with respect to reaction conditions, still need to be studied further. Ni was generally employed as the active metal while  $\text{CeO}_2$  was frequently used as the support in the RWGS reaction.<sup>34,37–39</sup> For instance, Wang *et al.*<sup>34,37,38</sup> synthesized Ni/ $\text{CeO}_2$  catalysts with careful control over preparation parameters, precipitants and Ni loading. Three kinds of Ni species were formed in Ni/ $\text{CeO}_2$  catalysts: Ni ions in a  $\text{CeO}_2$  lattice, highly dispersed Ni and bulk Ni. The highly dispersed Ni resulting from the oxygen vacancies is regarded as



David G. Evans studied as both an undergraduate and a research student at Jesus College, Oxford, and obtained a DPhil under the supervision of Prof. D. M. P. Mingos FRS. After postdoctoral work at Bristol University with Prof. F. G. A. Stone FRS, he was appointed as a lecturer at Exeter University in 1985. Several visits to Chinese university chemistry departments in the early 1990s

convinced him of China's great potential for development and he moved to Beijing University of Chemical Technology in 1996. His research interests focus on intercalation in layered solids.



Xue Duan was elected as an Academician of the Chinese Academy of Sciences in 2007. He was awarded his BS degree from the Jilin University and MS and PhD degrees from the Beijing University of Chemical Technology (BUCT). He was subsequently appointed to the staff of BUCT and established the Applied Chemistry Research Institute in 1990. He was promoted to full Professor in

1993 and given PhD supervisor status in 1995. He is currently Director of the Institute of Applied Chemistry and Executive Vice-Chair of the Academic Committee of the State Key Laboratory of Chemical Resource Engineering.

Table 1 Comparison of activities of the RWGS reaction

Catalyst	Preparation	WHSV (mL g <sup>-1</sup> h <sup>-1</sup> )	T/K	X <sub>CO<sub>2</sub></sub> (%)	Ref.
CuZnAl	Deposition-precipitation	n/a <sup>a</sup>	513	15	28
Cu + K/SiO <sub>2</sub>	Impregnation	300 000	873	12.8	29
Cu + Fe/SiO <sub>2</sub>	Impregnation	60 000	873	15	30
Fe nanoparticles	Fe-oxide deposition	6000	873	31	31
Fe-Mo/Al <sub>2</sub> O <sub>3</sub>	Deposition-precipitation	30 000	873	34	32
Pt/TiO <sub>2</sub>	Impregnation	12 000	873	49	33
Ni/CeO <sub>2</sub>	Deposition-precipitation	120 000	873	35	34
Ni/Ce-Zr-O	Impregnation	10 000	1023	49.7	35

<sup>a</sup> n/a: not available.

the key active component for the RWGS reaction, while the bulk Ni is responsible for CO<sub>2</sub> methanation. This result shows a prominent particle-size effect on reaction selectivity, which was reported by Wu *et al.*<sup>40</sup> In addition, CO<sub>2</sub> methanation can be inhibited by using Au or Cu as the main active metal as a result of a change in reaction pathway.<sup>41,42</sup> An Ni/CeO<sub>2</sub> catalyst prepared by using the co-precipitation method with a mixed precipitant (Na<sub>2</sub>CO<sub>3</sub>/NaOH = 1/1) and 2 wt% Ni loading exhibits the highest catalytic activity and longest life. Interestingly, the TPR results indicate a strong metal-support interaction (SMSI) between NiO particles and CeO<sub>2</sub> in the Ni/CeO<sub>2</sub> catalyst prepared by the impregnation method. The SMSI leads to the decoration of Ni particles by CeO<sub>x</sub> species, which induces a low activity in this catalyst toward CO<sub>2</sub> hydrogenation. These results demonstrate that CeO<sub>2</sub> as a support promotes the textural properties and stability of Ni catalysts (*e.g.*, high dispersion, good exposure and long-term stability) in the RWGS reaction.

### CeO<sub>2</sub> as active site

In addition to serving as a support, CeO<sub>2</sub> and CeO<sub>2</sub>-containing materials are recognized as active sites in the RWGS reaction.<sup>43,44</sup> Although the detailed mechanism is still uncertain, it is clear that the catalytic behavior of CeO<sub>2</sub> relies on its ability in creating oxygen vacancies and redox cycling between Ce<sup>4+</sup> and Ce<sup>3+</sup>. The oxygen vacancies and surface Ce species act as effective oxygen storage/release sites for redox catalysis. Zonetti *et al.*<sup>43</sup> prepared Ni<sub>x</sub>Ce<sub>0.75</sub>Zr<sub>0.25-x</sub>O<sub>2</sub> (NiCeZr) solid solution, Ce<sub>0.75</sub>Zr<sub>0.25</sub>O<sub>2</sub> (CeZr) and CeO<sub>2</sub> samples and evaluated them in the RWGS reaction. By correlating the catalytic activity and reducibility of these catalysts, the authors inferred that a stronger reducibility in the mixed oxide results in a higher activity in this reaction. After CO<sub>2</sub> chemisorption at room temperature for 1 h, a temperature programmed surface reaction (TPSR) was performed to detect the desorbed gases (*e.g.*, CO, H<sub>2</sub>O, CH<sub>4</sub> and CO<sub>2</sub>) from 25 to 700 °C in a H<sub>2</sub>/He flow. As shown in Fig. 1, a significantly higher CO selectivity and lower CH<sub>4</sub> selectivity are obtained over an NiCeZr catalyst (Fig. 1A) relative to the other two supported Ni catalysts (Ni/CeZr and Ni/NiCeZr in Fig. 1B and C, respectively), showing the significantly different catalytic performance of NiCeZr compared with supported Ni catalysts. Moreover, in the NiCeZr solid solution,

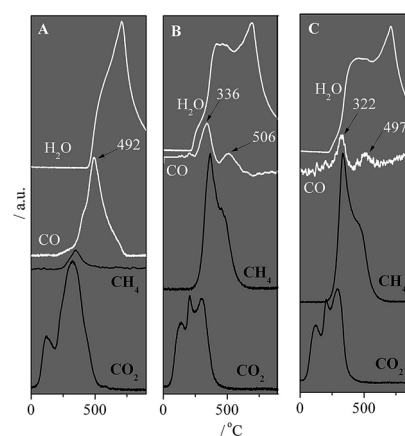


Fig. 1 TPSR profiles of catalysts:  $m/z = 44$  (CO<sub>2</sub>), 28 (CO), 15 (CH<sub>4</sub>) and 18 (H<sub>2</sub>O). (A) NiCeZr: the spectrum related to CO<sub>2</sub> is divided by 2, H<sub>2</sub>O divided by 6 and CO divided by 2. (B) Ni/CeZr: the spectrum related to CO<sub>2</sub> is divided by 2, H<sub>2</sub>O divided by 6, CO multiplied by 6 and CH<sub>4</sub> divided by 2. (C) Ni/NiCeZr: the spectrum related to CO<sub>2</sub> is divided by 2, H<sub>2</sub>O divided by 6, CO multiplied by 6 and CH<sub>4</sub> multiplied by 2. Reprinted with permission from ref. 43. Copyright 2014, Elsevier.

the incorporation of Ni into the lattice of CeZr oxide was demonstrated by Raman measurements: the peak of NiCeZr oxide shifts to 260 cm<sup>-1</sup> compared with that of CeZr oxide at 290 cm<sup>-1</sup>. Both the CeZr and CeO<sub>2</sub> samples without Ni successfully catalyze the CO<sub>2</sub> conversion, confirming that CeO<sub>2</sub> can play the role of active site in this reaction. Moreover, the NiCeZr catalyst is almost inactive in the cyclohexane dehydrogenation reaction, when metallic Ni is excluded from the catalyst surface. This work therefore demonstrates that CeO<sub>2</sub>-based mixed oxides, rather than Ni, act as the active sites toward the RWGS reaction.

### Catalytic mechanism

Understanding the reaction mechanism of the RWGS reaction is also valuable for the WGS reaction due to the principle of microscopic reversibility. With the development of advanced research techniques, studying the catalytic mechanism under *operando* conditions has become a hot topic in recent decades. However, how to reasonably apply the characterization techniques under *operando* conditions still causes controversy

and needs to be further explored. Meunier *et al.*<sup>45–47</sup> reported significantly different results concerning the reactivity of surface intermediates between *in operando* and *ex operando* conditions. They found that formate on the surface of a Pt/CeO<sub>2</sub> catalyst diminishes more quickly than carbonate and carbonyl in an Ar atmosphere. However, this happens much more slowly than with carbonate and carbonyl under true reaction conditions in an isotopic exchange experiment. This difference is probably due to the relationship between the desorption features of these intermediates and the oxidation state of CeO<sub>2</sub> in different atmospheres, which clearly shows the need to determine the reactivity of surface species under *operando* conditions. Their following work<sup>48</sup> employed a single reactor, which was monitored by diffuse reflectance FT-IR (DRIFT) and mass spectrometry (MS) using a steady-state isotopic transient kinetic analysis (SSITKA) technique to explore the reaction mechanism *in operando*. The parameter  $\tau$  represents the time at which the signal of each species decreased by 50% following the isotopic switch. For the surface species (carbonyl, carbonate or formate) and the reaction product (CO), the  $\tau$  values were measured by DRIFT and MS, respectively. They found that surface formate is not the main reaction intermediate for the formation of CO over Pt/CeO<sub>2</sub> catalysts; surface carbonate species adsorbed on the CeO<sub>2</sub> surface is shown to be the main surface intermediate (Fig. 2) while reaction through carbonyls adsorbed on the Pt surface is a minor route. This work provides a good example to explore the reaction mechanism of a complex catalytic system with multiple activity sites using an *in operando* technique.

However, Jacobs *et al.*<sup>49</sup> drew a completely different conclusion about the reaction intermediates for the RWGS reaction. They reported that the exchange rate of formate in a steady-state isotope-switching study greatly depends on whether water is introduced into the reaction gas. For this reason, the autocatalysis of water in the RWGS and WGS reactions cannot be neglected. In addition, their study on switching from <sup>12</sup>CO<sub>2</sub> to <sup>13</sup>CO<sub>2</sub> showed that surface carbonates and carbonyl exchange rapidly even in the absence of H<sub>2</sub>. This indicates that the fast exchange of surface carbonates and carbonyl is not due to the

reaction process but results from other reasons, such as thermal desorption.

Although valuable insights into the mechanism of the RWGS reaction and different surface intermediates were obtained from the transient kinetic technique, temporal analysis of products (TAP) measurements could provide more information related to reversible structural changes in the catalyst using alternating pulses of reducing gas and oxidizing gas.<sup>50,51</sup> Recently, a pulse-response TAP technique was applied to investigate the RWGS reaction on an Au/CeO<sub>2</sub> catalyst. The results showed that a surface-reduced Au/CeO<sub>2</sub> catalyst can be partially re-oxidized by exposure to CO<sub>2</sub> pulses. In addition, the surface oxygen deposited by CO<sub>2</sub> can be reactively removed again, which is significantly easier than removing that deposited by exposure to O<sub>2</sub>. In this work, the redox pathway on the Au surface or the interface between Au and CeO<sub>2</sub> was well illustrated with respect to the RWGS reaction. However, the catalyst structure of CeO<sub>2</sub> (*e.g.*, oxygen vacancies and surface hydroxyl), which is also sensitive to the atmosphere was not well considered in the reaction pathway.

In addition to the reaction mechanism, a study of the deactivation of CeO<sub>2</sub>-based catalysts in the WGS and RWGS reactions is also necessary for further improving the catalytic performance. Goguet *et al.*<sup>52</sup> investigated the deactivation rules of Pt/CeO<sub>2</sub> under RWGS conditions *via* an accelerated ageing procedure. Total recovery of the initial activity was obtained after reoxidation of the catalyst exposed to CO; this showed that carbon deposition was solely responsible for deactivation, excluding metal sintering. In addition, the catalyst activities (1% CO<sub>2</sub>, 4% H<sub>2</sub>, 300 °C) were measured before and after exposure to CO, CO<sub>2</sub>, H<sub>2</sub> or CH<sub>4</sub> at 400 °C. Exposure to an increasing amount of CO leads to increased deposition of carbon, resulting in deactivation, while moderate or no deactivation is found on exposure to CO<sub>2</sub>, CH<sub>4</sub> or H<sub>2</sub>. Additional TPO demonstrates the carbonaceous deposits during the RWGS reaction. This work illustrates the origin of deactivation of CeO<sub>2</sub>-based catalysts in the RWGS reaction, which could provide criteria for the design of effective catalysts with stable activity.

### 3. Methanation of CO<sub>2</sub>

Catalytic hydrogenation of CO<sub>2</sub> to methane, also called the Sabatier reaction, is the most advantageous reaction with respect to thermodynamics ( $\Delta G_{298\text{ K}} = -130.8\text{ kJ mol}^{-1}$ ) among CO<sub>2</sub> conversion reactions. However, the reduction of fully oxidized carbon to methane is an eight-electron process with significant kinetic limitations.<sup>9,53</sup>



In addition to its application in eliminating CO<sub>2</sub> emission, this reaction may also be applied in the future with respect to manned space exploration on Mars by converting the Martian CO<sub>2</sub> atmosphere into methane and water for astronaut life-support systems.<sup>54</sup> The reaction mechanism of CO<sub>2</sub> methanation is normally classified into two categories: one involves CO

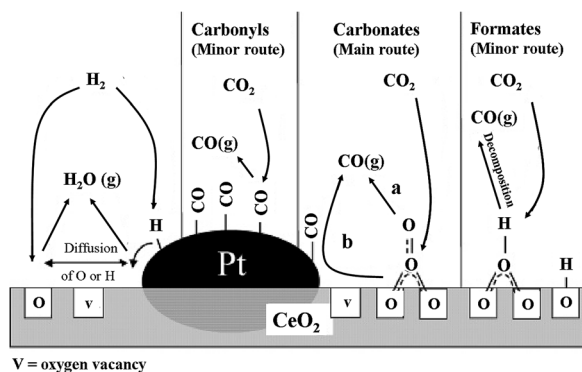


Fig. 2 Model for the mechanism of the RWGS reaction over Pt/CeO<sub>2</sub>. Reprinted with permission from ref. 48. Copyright 2004, American Chemical Society.

Table 2 Comparison of activities of CO<sub>2</sub> methanation

Catalyst	Preparation	WHSV/GHSV	T/K	X <sub>CO<sub>2</sub></sub> (%)	Ref.
Ni/γ-Al <sub>2</sub> O <sub>3</sub>	Impregnation	9000 mL g <sup>-1</sup> h <sup>-1</sup>	623	78	57
Ni/TiO <sub>2</sub>	Deposition-precipitation	2400 mL g <sup>-1</sup> h <sup>-1</sup>	533	96	58
Ni/β-zeolite	Impregnation	882 h <sup>-1</sup>	633	97	59
Ni/ZrO <sub>2</sub> -Al <sub>2</sub> O <sub>3</sub>	Impregnation-precipitation	8100 mL g <sup>-1</sup> h <sup>-1</sup>	633	69.8	60
Ru/SiO <sub>2</sub>	Impregnation	2400 mL g <sup>-1</sup> h <sup>-1</sup>	673	80	53
Ru/TiO <sub>2</sub>	Photohole-oxidation	2400 mL g <sup>-1</sup> h <sup>-1</sup>	493	99	53
Ru/Al <sub>2</sub> O <sub>3</sub>	n/a <sup>a</sup>	15 000 h <sup>-1</sup>	573	96	61
Ru/CeO <sub>2</sub>	Deposition-precipitation	2400 mL g <sup>-1</sup> h <sup>-1</sup>	523	94	20

<sup>a</sup> n/a: not available.

as the reaction intermediate, which then follows the mechanism of CO methanation;<sup>55</sup> the other involves some C-containing chemicals (*e.g.*, formate and carbonate) as intermediates, which directly hydrogenate without forming CO.<sup>56</sup> A series of catalysts have been developed for this reaction, in which CeO<sub>2</sub>-based material exhibited superior catalytic activity (Table 2).

### CeO<sub>2</sub> as support

Metal (*e.g.*, Ru and Ni) catalysts with CeO<sub>2</sub> as support are effective toward CO<sub>2</sub> methanation.<sup>62–65</sup> Tada *et al.*<sup>62</sup> prepared different metal oxides (CeO<sub>2</sub>, α-Al<sub>2</sub>O<sub>3</sub>, TiO<sub>2</sub> and MgO) to support Ni catalysts and carried out evaluation for CO<sub>2</sub> methanation. A Ni/CeO<sub>2</sub> sample showed the highest CO<sub>2</sub> conversion compared with the other catalysts, especially at low temperatures, which was attributed to the enhanced adsorption of CO<sub>2</sub>-derived species and the partial reduction of the CeO<sub>2</sub> surface. Doping CeO<sub>2</sub> with Zr (Ce<sub>x</sub>Zr<sub>1-x</sub>O<sub>2</sub>) is an effective approach to improve the reduction degree and the concentration of oxygen vacancies. Ocampo *et al.*<sup>63</sup> prepared several Ni/Ce<sub>0.72</sub>Zr<sub>0.28</sub>O<sub>2</sub> catalysts containing different Ni loadings and measured their catalytic activity in CO<sub>2</sub> methanation. The high oxygen storage capacity of Ce<sub>x</sub>Zr<sub>1-x</sub>O<sub>2</sub> and a high dispersion of Ni are believed to bring about the high performance of these catalysts. Ce<sub>x</sub>Zr<sub>1-x</sub>O<sub>2</sub>-supported Ni-Co bimetallic catalysts were also developed toward the methanation of both CO<sub>2</sub> and CO.<sup>64</sup> The metal-support interaction and the existence of oxygen vacancies play key roles in the catalytic performance. Although many metal catalysts supported on CeO<sub>2</sub> with high activity and stability have been reported, the origin of the good performance is attributed to several factors, which still needs to be clarified by confirming the active sites and the corresponding reaction mechanism.

### CeO<sub>2</sub> as active site

Generally speaking, a metal (*e.g.*, Ru or Ni) surface is supposed to be the active site for CO<sub>2</sub> methanation. However, it was reported that the metal oxide acts as the active site while the metal surface acts as the supplier of hydrogen in some cases.<sup>66–73</sup> Pan *et al.*<sup>66</sup> studied the CO<sub>2</sub> adsorption and methanation activity over Ce<sub>0.5</sub>Zr<sub>0.5</sub>O<sub>2</sub> and γ-Al<sub>2</sub>O<sub>3</sub>-supported nickel catalysts, respectively. Ce<sub>0.5</sub>Zr<sub>0.5</sub>O<sub>2</sub> provides unique medium basic sites for CO<sub>2</sub> adsorption and subsequent conversion to carbonate and monodentate formate, which undergo

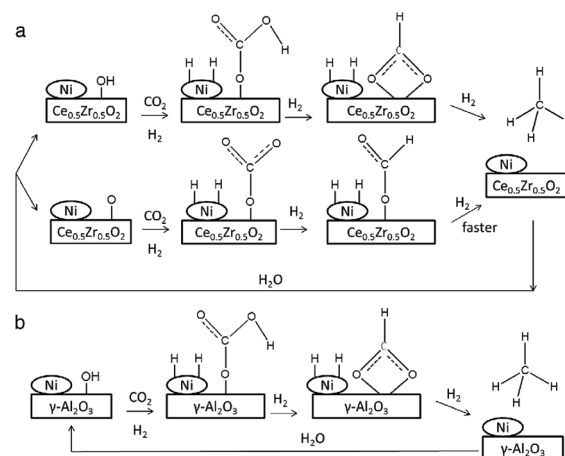


Fig. 3 Proposed pathways for CO<sub>2</sub> activation and methanation over (a) Ni/Ce<sub>0.5</sub>Zr<sub>0.5</sub>O<sub>2</sub> and (b) Ni/γ-Al<sub>2</sub>O<sub>3</sub>. Reprinted with permission from ref. 66. Copyright 2014, Elsevier.

hydrogenation more quickly than bidentate formate (Fig. 3). According to previous reports, the Ce<sup>3+</sup> sites are probably serving as the medium basic sites for CO<sub>2</sub> adsorption and conversion.<sup>21</sup> The bonding mode between Ce<sup>3+</sup> and C-containing species and their structural changes in the catalytic cycle still need to be explored in detail, which would largely promote understanding of the reaction mechanism of CO<sub>2</sub> over CeO<sub>2</sub>-based catalysts.

Leitenburg *et al.*<sup>67</sup> reported that the adsorption and activation of CO<sub>2</sub> occur on the surface Ce<sup>3+</sup> site, which converts to CO along with a valence change from Ce<sup>3+</sup> to Ce<sup>4+</sup>. The oxygen bulk vacancies play an important role in the reduction of CO<sub>2</sub> to CO and/or surface carbonaceous species, which then rapidly hydrogenate to CH<sub>4</sub> over the supported metal. In our recent work, the promoting effect of metal nanoparticles (Ru) on the formation of oxygen vacancies was clearly confirmed.<sup>20</sup> In addition, the surface oxygen vacancies on CeO<sub>2</sub> rather than Ru are more likely to be the active sites in CO<sub>2</sub> methanation, based on the quantitative relation between the reaction rate and concentration of surface oxygen vacancies. With respect to the reaction mechanism on oxygen vacancies, formate was proved to be the reaction intermediate by steady-state isotope transient kinetic analysis (SSITKA)-type *in situ* DRIFT infrared

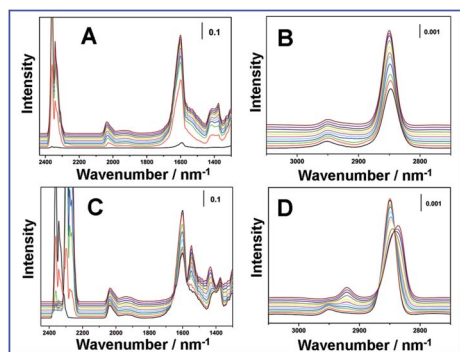


Fig. 4 (A and B) DRIFT spectra recorded at 150 °C during 90 min over the Ru(3%)/CeO<sub>2</sub>-NCs catalyst with <sup>12</sup>CO<sub>2</sub> as reaction gas; (C and D) subsequent reaction during 45 min by introducing <sup>13</sup>CO<sub>2</sub> as reaction gas. From bottom to top: (A and B) 0, 0.5, 2, 5, 10, 15, 20, 30, 50, 70, 90 min; (C and D) 0, 0.5, 1, 2, 4, 6, 10, 15, 20, 30, 45 min. Reprinted with permission from ref. 20. Copyright 2015, Elsevier.

spectroscopy, which is different from the generally recognized CO intermediate on a metal surface (Fig. 4).

Doping CeO<sub>2</sub> with noble metal is a promising route to prepare CeO<sub>2</sub>-based materials with abundant oxygen vacancies. Metiu *et al.*<sup>68</sup> prepared several CeO<sub>2</sub> catalysts doped with Ni, Co, Pd or Ru by the combustion method and evaluated them in CO<sub>2</sub> methanation. Among these catalysts, the reduced Ru-doped CeO<sub>2</sub> sample shows the best catalytic activity. The author reported that doping of Ru facilitates the reduction process at a lower temperature, which results in more oxygen vacancies. XRD and XPS were used to verify the crystal structure of the doped oxide (*e.g.*, Ce<sub>0.95</sub>Ru<sub>0.05</sub>O<sub>2</sub>) and the location of Ru in CeO<sub>2</sub> was studied using a calculation method. When the Ru atom is located in the second Ce layer, the energy is lower than that in the surface region. Although it is not possible for all the Ru atoms to enter into the subsurface layer, this result indicates that most of the Ru atoms cannot make contact with the reactants and act as active sites. In their recent work, Metiu *et al.*<sup>69</sup> further studied the oxidation state of the surface of an Ru-doped CeO<sub>2</sub> catalyst. The activity was found to be sensitive to the reduction degree of the catalyst surface; an over-oxidized or over-reduced surface leads to a decreased catalytic activity. This further verifies that the surface of CeO<sub>2</sub> provides active sites and its reduction degree greatly affects the reaction process.

According to the reports mentioned above, the superior catalytic performance of CeO<sub>2</sub> as active site is dependent on a unique reaction mechanism, which is different from that on a metal surface. Applying *operando* characterization techniques (*e.g.*, Raman, TEM, EXAFS and IR) would be a good strategy to obtain detailed structural information on active sites and reaction mechanisms under practical conditions.

## 4. Synthesis of methanol

Methanol is a common solvent and a key material in chemical industry due to its extensive use in synthesizing liquid fuels (*e.g.*, hydrocarbons and dimethylether). As an alternative feedstock for synthesis gas (CO), converting CO<sub>2</sub> into methanol is a promising process for large-scale application.<sup>74</sup>



The thermodynamic features of this reaction favor a low reaction temperature and a high reaction pressure. However, the difficulty in CO<sub>2</sub> activation requires an enhanced temperature to achieve an acceptable reaction rate.<sup>75</sup> Just like the CO<sub>2</sub> methanation, two categories of reaction mechanism are in debate so far: one involves CO as intermediate, which is produced *via* the RWGS reaction and then hydrogenates to methanol following the conventional syngas-to-methanol conversion (CO + H<sub>2</sub> → CH<sub>3</sub>OH).<sup>76,77</sup> The other has formate or carbonate as the intermediate, which originates from the adsorption and hydrogenation of CO<sub>2</sub>.<sup>78,79</sup> Various types of catalyst have been developed for the RWGS reaction (Table 3). Among these, CeO<sub>2</sub>-based materials have aroused intensive interest in recent years and have exhibited superior catalytic activity.

### CeO<sub>2</sub> as support

In the work of Yang *et al.*,<sup>86</sup> the support effect of CeO<sub>2</sub> on an Au/TiO<sub>2</sub> catalyst was carefully studied in the synthesis of methanol from CO<sub>2</sub>. DFT calculation was applied to study the electronic metal-support interaction at the Au<sub>3</sub>-CeO<sub>x</sub> interface (Fig. 5A). The significant charge redistribution of Au atoms would promote binding of the positively charged carbon of CO<sub>2</sub> to Au<sup>δ-</sup> and the negatively charged oxygen to Ce<sup>δ+</sup>. DFT calculations were also performed to optimize the potential energy

Table 3 Comparison of activities in synthesis of methanol

Catalyst	Preparation	WHSV/GHSV	T/K	X <sub>CO<sub>2</sub></sub> (%)	S <sup>a</sup> (%)	Ref.
Cu/ZrO <sub>2</sub>	Deposition-precipitation	5400 h <sup>-1</sup>	513	6.3	48.8	80
Cu-Zn/ZrO <sub>2</sub>	Coprecipitation	3300 h <sup>-1</sup>	493	21.0	68.0	81
Ag-Zn/ZrO <sub>2</sub>	Coprecipitation	3300 h <sup>-1</sup>	493	2.0	97.0	81
Au-Zn/ZrO <sub>2</sub>	Coprecipitation	3300 h <sup>-1</sup>	493	1.5	100	81
Cu-Ga/ZnO	Co-impregnation	18 000 mL g <sup>-1</sup> h <sup>-1</sup>	543	6.0	88.0	82
Cu-Zn-Al/ZrO <sub>2</sub>	Coprecipitation	9742 h <sup>-1</sup>	513	18.7	47.2	83
Pd-Zn/CNTs	Incipient wetness	1800 mL g <sup>-1</sup> h <sup>-1</sup>	523	6.3	99.6	84
LaCr <sub>0.5</sub> Cu <sub>0.5</sub> O <sub>3</sub>	Sol-gel	9000 mL g <sup>-1</sup> h <sup>-1</sup>	523	10.4	90.8	85

<sup>a</sup> Selectivity of methanol.

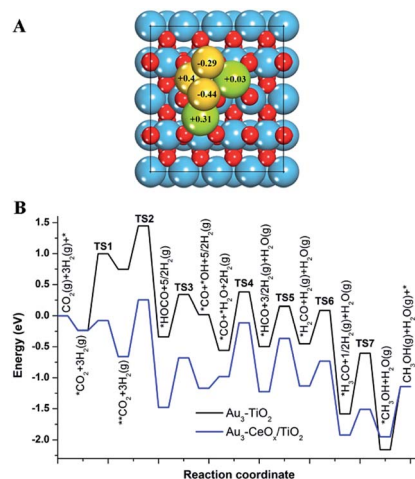


Fig. 5 Charge transfer and reaction energetics calculated by DFT. (A) The net Bader charges of Au and Ce. +, electron loss; −, electron gain. (B) DFT-optimized potential energy surface (PES) for CO<sub>2</sub> hydrogenation on Au<sub>3</sub>/TiO<sub>2</sub>(110) and Au<sub>3</sub>/CeO<sub>x</sub>/TiO<sub>2</sub>(110). "TS" corresponds to transition state. Reprinted with permission from ref. 86. Copyright 2015, American Chemical Society.

surface (PES) in this reaction on Au<sub>3</sub>/TiO<sub>2</sub>(110) and Au<sub>3</sub>/CeO<sub>x</sub>/TiO<sub>2</sub>(110) (Fig. 5B). The results reveal that Au<sub>3</sub> supported on CeO<sub>x</sub>/TiO<sub>2</sub>(110) decreases the reaction barriers for CO and methanol production, which allows Au to hydrogenate CO<sub>2</sub> with an unprecedentedly low hydrogen pressure. Ambient-pressure X-ray photoelectron spectroscopy (AP-XPS) was also used to confirm the unique surface electronic properties and the CO<sub>2</sub> activation mechanism at the active Au–CeO<sub>x</sub> interface. The results show that the activation of CO<sub>2</sub> requires both metallic Au and Ce<sup>3+</sup>. For this reason, the interfacial region between metallic Au and Ce<sup>3+</sup> is the most favourable adsorption site in this reaction. The experimental-theoretical combined study was well demonstrated in this study, which revealed a detailed correlation between the catalyst structure and catalytic activity. However, the methanol selectivity over the Au/TiO<sub>2</sub>CeO<sub>2</sub> catalyst was below 1%, which is significantly lower than that for the CuZnAl catalyst (above 40%) and still needs to be improved.

### CeO<sub>2</sub> as active site

Bonura *et al.*<sup>87</sup> studied the catalytic role of CeO<sub>2</sub> in Cu/ZnO and Cu/ZrO<sub>2</sub> catalysts toward CO<sub>2</sub> hydrogenation to methanol. As the CeO<sub>2</sub> content increases, both the specific surface area and metal dispersion decrease, indicating that CeO<sub>2</sub> is not good for promoting the textural properties of Cu catalysts compared with ZrO<sub>2</sub>. However, the CeO<sub>2</sub>-containing catalysts exhibit much higher methanol yields in comparison with those without CeO<sub>2</sub>. The metal surface is not the only active site, due to the lack of relationship between metal surface and catalytic activity. This to some extent confirms the fundamental role of the metal/oxide interface as the active site. Arena *et al.*<sup>88</sup> obtained a similar conclusion in their research on the promoting effect of Al<sub>2</sub>O<sub>3</sub>, ZrO<sub>2</sub> and CeO<sub>2</sub> on the Cu/ZnO system in the synthesis of methanol *via* CO<sub>2</sub> hydrogenation. They reported that, although

CeO<sub>2</sub> shows a weaker promoting effect on the texture of the Cu/ZnO system, the CuZnCe catalyst displays a more than twofold larger methanol yield owing to its high selectivity level over the whole reaction temperature range. These two exploratory studies introduced CeO<sub>2</sub> into the traditional Cu/ZnO catalyst, offering a new strategy to obtain promising catalytic activity and selectivity toward CO<sub>2</sub> hydrogenation to methanol. However, due to the complexity of the catalyst system, the exact role of CeO<sub>2</sub> in this reaction is not fully understood.

As an alternative to the traditional Cu/ZnO catalysts, Graciani *et al.*<sup>21</sup> reported highly active Cu–CeO<sub>2</sub> and Cu–CeO<sub>2</sub>–TiO<sub>2</sub> catalysts for the synthesis of methanol from CO<sub>2</sub>. The experimental results and theoretical calculation indicated a different type of active site for CO<sub>2</sub> activation at the Cu–CeO<sub>2</sub> interface, which was highly efficient for the synthesis of methanol. The combination of metal and oxide at the Cu–CeO<sub>2</sub> interface leads to a special reaction pathway (COOH rather than formate as the reaction intermediate) for this reaction. The different reaction pathways resulting from different active sites induce a significantly higher rate of methanol production on CeO<sub>x</sub>/Cu(111), which is ~200 and ~14 times faster than on Cu(111) and Cu/ZnO(0001), respectively. Furthermore, the apparent activation energy for methanol synthesis (calculated by DFT calculation) is 12 kcal mol<sup>−1</sup> on CeO<sub>x</sub>/Cu(111), which is lower than that on Cu(111) and Cu/Zn(0001) (25 and 16 kcal mol<sup>−1</sup>, respectively). This is the first investigation of Cu–CeO<sub>x</sub> catalysts toward the synthesis of methanol, which makes good use of DFT calculations for reaction simulation at the Cu–CeO<sub>x</sub> interface. The result is very impressive and will encourage further work in this field.

## 5. CO<sub>2</sub> reforming of methane

CO<sub>2</sub> reforming of methane, the so-called dry reforming of methane (DRM), is an interesting route to convert CO<sub>2</sub> and CH<sub>4</sub> (another green house gas) to synthesis gas.<sup>89,90</sup> Compared with partial oxidation and steam reforming, the H<sub>2</sub>/CO ratio of the synthesis gas obtained from the DRM reaction is close to 1 : 1, which is appropriate for further use in the production of oxygenated compounds as well as Fischer–Tropsch synthesis for liquid hydrocarbon production.<sup>91</sup>



The DRM reaction mechanism is considered to involve two independent steps: the first step is the decomposition of CH<sub>4</sub> to carbon and H<sub>2</sub> on the metal surface; the second is the combination of carbon with oxygen to produce CO.<sup>92–94</sup> Since the DRM reaction is a strongly endothermic reaction, a high temperature favors a high conversion. Wang *et al.*<sup>95</sup> reported that the DRM reaction generally proceeds at temperatures in excess of 913 K. The main problems in this reaction are coke deposition and sintering of metal nanoparticles, which cause severe deactivation of catalysts. As a promising resolution, CeO<sub>2</sub> can act as a source of active oxygen species that originates from CO<sub>2</sub>. This will effectively scavenge and gasify the coke forming over the catalyst.<sup>96–102</sup> Moreover, the CeO<sub>2</sub> substrate interacts strongly

Table 4 Activities and coke formation rates of various catalysts for the DRM reaction

Catalyst	WHSV/gas flow rate	T/K	X <sub>CH<sub>4</sub></sub> (%)	X <sub>CO<sub>2</sub></sub> (%)	Coke formation (wt%)	Ref.
Ni/alumina aerogel	48 000 mL g <sup>-1</sup> h <sup>-1</sup>	973	66	71	250 μmol g <sup>-1</sup> h <sup>-1</sup>	103
Ni/SiC	6000 mL g <sup>-1</sup> h <sup>-1</sup>	1023	92	93	n/a <sup>a</sup>	104
NiO/CaO	50 000 mL g <sup>-1</sup> h <sup>-1</sup>	1123	95	n/a	n/a	105
Ni-Co/Al <sub>2</sub> O <sub>3</sub>	91.7 mL min <sup>-1</sup>	1023	90	n/a	0.001	106
Ni-Mn/Al <sub>2</sub> O <sub>3</sub>	91.7 mL min <sup>-1</sup>	1023	95	n/a	0.006	106
Ru/MgO	107 500 mL g <sup>-1</sup> h <sup>-1</sup>	1023	39	44	1.2	107
Ru/Al <sub>2</sub> O <sub>3</sub>	107 500 mL g <sup>-1</sup> h <sup>-1</sup>	1023	35	39	19.5	107
Ru/SiO <sub>2</sub>	107 500 mL g <sup>-1</sup> h <sup>-1</sup>	1023	20	23	16.4	107
Ru/TiO <sub>2</sub>	107 500 mL g <sup>-1</sup> h <sup>-1</sup>	1023	28	30	ND <sup>b</sup>	107

<sup>a</sup> n/a: not available. <sup>b</sup> ND: not detected.

with the supported metal nanoparticles to overcome their agglomeration. A series of catalysts has been developed for this reaction and among these, a CeO<sub>2</sub>-based material exhibited superior catalytic activity (Table 4).

### CeO<sub>2</sub> as support

Ni particles with sizes of several nanometers have been proven to be able to suppress carbon deposition during methane reforming. In order to control the particle size of Ni with the confinement effect of SBA-16, Zhang *et al.*<sup>96</sup> prepared Ni/SBA-16 and Ni/SBA-16 modified with equimolar CeO<sub>2</sub> relative to Ni (denoted as NiCe/SBA-16) and applied them in DRM reactions. The CO<sub>2</sub> and methane conversions at 973 K on NiCe/SBA-16 are more stable than those on Ni/SBA-16 over a 100 h reaction period. XRD, Raman spectra and TPH experiments clearly showed less carbon deposition with NiCe/SBA-16 compared with that with Ni/SBA-16 after the reaction. Moreover, a more uniform Ni particle size was observed by HRTEM for NiCe/SBA-16 relative to Ni/SBA-16 (Fig. 6). These two factors account for the high stability of NiCe/SBA-16 in the DRM reaction.

Wang *et al.*<sup>97</sup> found that CeO<sub>2</sub> has a positive effect on catalytic activity, stability and carbon suppression in this reaction when it is used as a promoter for Ni/γ-Al<sub>2</sub>O<sub>3</sub>. When CeO<sub>2</sub> alone is used as a support for Ni catalysts, however, it exhibits too strong a metal-support interaction, which reduces the catalytic

activity. Roh *et al.*<sup>98</sup> employed a co-precipitation method to prepare ZrO<sub>2</sub>, CeO<sub>2</sub> and cubic Ce<sub>0.8</sub>Zr<sub>0.2</sub>O<sub>2</sub>-supported Ni catalysts, which were evaluated in the CO<sub>2</sub> methane-reforming reaction. The Ni/ZrO<sub>2</sub> catalyst deactivates at the initial stage of the reaction due to serious carbon deposition. In contrast, the samples of Ni/CeO<sub>2</sub> and Ni/Ce<sub>0.8</sub>Zr<sub>0.2</sub>O<sub>2</sub> exhibit a high catalytic activity (CH<sub>4</sub> conversion > 95% at 800 °C) during the reaction. The largely enhanced catalytic performance is attributed to the intimate contact between metal and support, which results in an improved Ni dispersion and the suppression of carbon formation. The strong metal-support interaction in the Ni/CeO<sub>2</sub> system was also studied from the viewpoint of Ni morphology. Gonzalez-DelaCruz *et al.*<sup>99</sup> found that the state of nickel in a Ni/CeO<sub>2</sub> catalyst is dependent on the atmosphere by means of *in situ* XAS spectroscopy. The nickel particles are flattened and strongly stabilized on the partially reduced CeO<sub>2</sub> surface under strongly reducing conditions, which accounts for the enhanced stability observed for the CO<sub>2</sub> reforming of CH<sub>4</sub> compared with steam reforming of CH<sub>4</sub> (Fig. 7). A similar conclusion was also obtained with respect to Pt catalysts supported on nanocrystalline mesoporous ZrO<sub>2</sub> and CeO<sub>2</sub>-ZrO<sub>2</sub> carriers:<sup>100</sup> the pre-treatment temperature and the concentration of CeO<sub>2</sub> impose a great influence on the morphology of Pt particles. The high

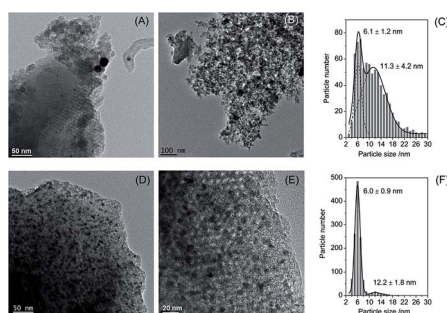


Fig. 6 TEM images of (A and B) the used Ni/SBA-16 and (D and E) used NiCe/SBA-16 after catalytic reactions at 973 K for 100 h, with Ni particle size distributions for (C) the used Ni/SBA-16 and (F) used NiCe/SBA-16 catalyst. Reprinted with permission from ref. 72. Copyright 2015, American Chemical Society.

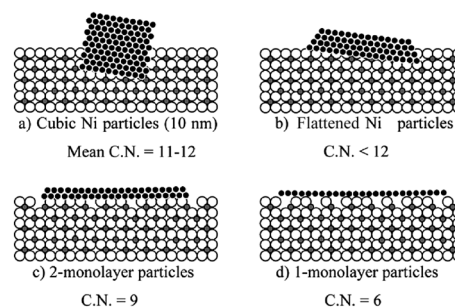


Fig. 7 Schematic evolution of the shape of the metallic nickel particles submitted to a reducing treatment up to 750 °C. By high temperature reduction, the nickel spread onto the partially reduced surface of CeO<sub>2</sub>. The mean coordination number of nickel strongly depends on the shape: (a) in the 11–12 range for the cubic 10 nm particles, (b) <12 for the flattened Ni particles, (c) 9 for the two-monolayer particles, (d) 6 for the one-monolayer particles. Reprinted with permission from ref. 99. Copyright 2008, Elsevier.

stability of Pt/CeO<sub>2</sub>-ZrO<sub>2</sub> catalysts is related to the close contact between Pt and CeO<sub>2</sub>.

Although CeO<sub>2</sub>-based catalysts have shown good catalytic performance in the DRM reaction, further development of superior catalysts (stable, active and selective) is urgently needed to satisfy the demands of industrial application. More efforts have to be made in the design of heterogeneous catalysts to overcome the coke deposition and sintering of metal nanoparticles mentioned above. Coke deposition is the main obstacle with respect to the DRM reaction. The high reaction rate of methane activation over the metal clusters results in excessive coke production, which cannot be gasified in time due to the lack of a traditional strong oxidant (e.g., O<sub>2</sub> in the partial oxidation of methane (POM) and steam in the steam reforming of methane (SRM)). For this reason, a rational catalyst should strike a balance between these two elementary reactions. Decreasing the activity of a metal catalyst (predominantly nickel) for C-H bond cleavage is a promising method. On the other hand, the synthesis of appropriate CeO<sub>2</sub>-based materials toward increased coke gasification is also helpful. Pinter *et al.* successfully reduced the coke deposition with a bimetallic catalyst supported on CeO<sub>2</sub>-ZrO<sub>2</sub> mixed oxides, such as CoFe, CoW, NiFe and NiW pairs.<sup>108-110</sup> In their following work, the sintering of metal nanoparticles was also well-resolved by introducing a refractory secondary support (ordered mesoporous alumina or silicon), so as to minimize the spatial segregation of active components and maintain a large metal cluster-support interface.<sup>108,111,112</sup> By employing these approaches simultaneously, stable catalytic operation with no coke accumulation has been achieved over extended time periods.

## 6. Conclusions

This *Overview Article* summarizes the recent progress in the design and preparation of CeO<sub>2</sub>-based materials as heterogeneous catalysts toward CO<sub>2</sub> conversion reactions, including the RWGS reaction, CO<sub>2</sub> methanation, synthesis of methanol from CO<sub>2</sub> and CO<sub>2</sub> reforming of methane. By virtue of the abundant surface oxygen vacancies and reversible valence change between Ce<sup>4+</sup> and Ce<sup>3+</sup>, a great number of heterogeneous catalysts with high dispersion and stability have been reported, exhibiting good catalytic activity and long service life. However, several key issues, including high reaction temperature, low CO<sub>2</sub> conversion and unsatisfactory selectivity, are still not well resolved with respect to the demands of industrial application. In order to rationally develop advanced catalysts with high performance, deepening the following basic understanding of catalysis science in this area is highly necessary: (i) it is difficult to clearly identify the active site structure (e.g., the metal surface, oxygen vacancy, Ce<sup>3+</sup> or metal-support interface), which inevitably restricts rational design and precise control over catalyst microstructure; (ii) although CeO<sub>2</sub>-based catalysts show good catalytic activity and stability in these reactions, the intrinsic catalytic mechanism has not been well understood to date.

In order to resolve the problems mentioned above, the following four proposed strategies would be helpful. Firstly, an

accurate correlation between the reaction activity and different structural centers is a useful method. Quantitative exploration of the reaction rate as a function of individual numbers of possible active sites would provide a feasible strategy to reveal the true active site. This is challenging since the catalyst structure and number of active sites must be tuned very precisely and carefully, otherwise a wrong relationship would be obtained. In principle, the determination of an intrinsic active site can be implemented through passivating a specific structural unit/group by an inert agent followed by a systematic evaluation of catalytic performance. A series of such control experiments can disclose a true structure-property correlation. Secondly, investigations of catalytic mechanisms over a CeO<sub>2</sub>-based heterogeneous catalyst are always attractive but difficult, especially in a multi-step and structure-sensitive reaction system. A different active site is likely to induce a different reaction route, intermediate and selectivity, which results in a rather complicated catalytic mechanism. In this case, building up a model catalytic system (e.g., defined crystal plane or atomic arrangement by chemical vapor deposition or the hydrothermal synthesis method) would eliminate unnecessary interference and simplify the study procedure. More importantly, applying *operando* characterization techniques (e.g., Raman, TEM, EXAFS and IR) would obtain detailed structural information on active sites and reaction mechanisms under practical conditions. If an intimate correlation between the reversible structural change of the catalyst and the state variation of the reactive agent is obtained by combined *operando* techniques, the active site-dependent reaction mechanism can be fully described. Finally, theoretical calculations have been recognized as a powerful method to simulate the reaction mechanism on a defined catalytic active site, which provides a supplementary or even indispensable approach in addition to experimental studies. With the rapid advance of characterization techniques and good understanding of structure-activity relationships, the rational design and controllable preparation of CeO<sub>2</sub>-based catalysts would make an effective contribution toward CO<sub>2</sub> conversion. From the viewpoint of industrial utilization, the RWGS and DRM reactions are promising strategies for syngas production. For the synthesis of methanol from CO<sub>2</sub>, however, more work is urgently needed due to the unsatisfactory catalytic performance.

## Acknowledgements

This work was supported by the National Natural Science Foundation of China (NSFC), the 973 Program (Grant No. 2014CB932104) and the Specialized Research Fund for the Doctoral Program of Higher Education (20130010110013). M. Wei particularly appreciates the financial aid from the China National Funds for Distinguished Young Scientists of the NSFC.

## Notes and references

- 1 M. A. A. Aziz, A. A. Jalil, S. Triwahyono and A. Ahmad, *Green Chem.*, 2015, 17, 2647.

- 2 D. Ma, B. Li, K. Liu, X. Zhang, W. Zou, Y. Yang, G. Li, Z. Shi and S. Feng, *J. Mater. Chem. A*, 2015, **3**, 23136.
- 3 C. S. Song, *Catal. Today*, 2006, **115**, 2.
- 4 W. Wang, S. Wang, X. Ma and J. Gong, *Chem. Soc. Rev.*, 2011, **40**, 3703.
- 5 S. Wang, W. Yao, J. Lin, Z. Ding and X. Wang, *Angew. Chem., Int. Ed.*, 2014, **53**, 1034.
- 6 R. Kuriki, K. Sekizawa, O. Ishitani and K. Maeda, *Angew. Chem., Int. Ed.*, 2015, **54**, 2406.
- 7 S. Wang and X. Wang, *Angew. Chem., Int. Ed.*, 2016, **55**, 2308.
- 8 W. C. Chueh, C. Falter, M. Abbott, D. Scipio, P. Furler, S. M. Haile and A. Steinfeld, *Science*, 2010, **330**, 1797.
- 9 J. N. Park and E. W. McFarland, *J. Catal.*, 2009, **266**, 92.
- 10 F. Esch, S. Fabris, L. Zhou, T. Montini, C. Africh, P. Fornasiero, G. Comelli and R. Rosei, *Science*, 2005, **309**, 752.
- 11 C. T. Campbell and C. H. F. Peden, *Science*, 2005, **309**, 713.
- 12 Y. Li, X. He, J. Yin, Y. Ma, P. Zhang, J. Li, Y. Ding, J. Zhang, Y. Zhao, Z. Chai and Z. Zhang, *Angew. Chem., Int. Ed.*, 2015, **54**, 1832.
- 13 Y. Wang, F. Wang, Y. Chen, D. Zhang, B. Li, S. Kang, X. Li and L. Cui, *Appl. Catal., B*, 2014, **147**, 602.
- 14 J. Jiao, Y. Wei, Z. Zhao, J. Liu, J. Li, A. Duan and G. Jiang, *Ind. Eng. Chem. Res.*, 2014, **53**, 17345.
- 15 B. Zhao, Y. Pan and C. Liu, *Catal. Today*, 2012, **194**, 60.
- 16 N. Ta, J. Liu, S. Chenna, P. A. Crozier, Y. Li, A. Chen and W. Shen, *J. Am. Chem. Soc.*, 2012, **134**, 20585.
- 17 N. Acerbi, S. C. E. Tsang, G. Jones, S. Golunski and P. Collier, *Angew. Chem., Int. Ed.*, 2013, **52**, 7737.
- 18 H. Yen, Y. Seo, S. Kaliaguine and F. Kleitz, *Angew. Chem., Int. Ed.*, 2012, **51**, 12032.
- 19 A. Trovarelli, *Catal. Rev.*, 1996, **38**(4), 439.
- 20 F. Wang, C. Li, X. Zhang, M. Wei, D. G. Evans and X. Duan, *J. Catal.*, 2015, **329**, 177.
- 21 J. Graciani, K. Mudiyansele, F. Xu, A. E. Baber, J. Evans, S. D. Senanayake, D. J. Stacchiola, P. Liu, J. Hrbek, J. F. Sanz and J. A. Rodriguez, *Science*, 2014, **345**, 6196.
- 22 A. Corma and H. Garcia, *J. Catal.*, 2013, **308**, 168.
- 23 S. H. Hakim, C. Sener, A. C. Alba-Rubio, T. M. Gostanian, B. J. O'Neill, F. H. Ribeiro, J. T. Miller and J. A. Dumesic, *J. Catal.*, 2015, **328**, 75.
- 24 G. Centi, G. Iaquaniello and S. Perathoner, *ChemSusChem*, 2011, **4**, 1265.
- 25 G. Centi and S. Perathoner, *Catal. Today*, 2009, **148**, 191.
- 26 M. J. L. Ginés, A. J. Marchi and C. R. Apesteguía, *Appl. Catal., A*, 1997, **154**, 155.
- 27 C. S. Chen, W. H. Cheng and S. S. Lin, *Appl. Catal., A*, 2003, **238**, 55.
- 28 F. S. Stone and D. Waller, *Top. Catal.*, 2003, **22**, 305.
- 29 C. Chen, W. Cheng and S. Lin, *Appl. Catal., A*, 2003, **238**, 55.
- 30 C. Chen, W. Cheng and S. Lin, *Chem. Commun.*, 2001, **37**, 1770.
- 31 D. H. Kim, S. W. Han, H. S. Yoon and Y. D. Kim, *J. Ind. Eng. Chem.*, 2015, **23**, 67.
- 32 A. G. Kharaji, A. Shariati and M. A. Takassi, *Chin. J. Chem. Eng.*, 2013, **21**, 1007.
- 33 S. S. Kim, H. H. Lee and S. C. Hong, *Appl. Catal., B*, 2012, **119–120**, 100.
- 34 L. Wang, H. Liu, Y. Liu, Y. Chen and S. Yang, *J. Rare Earths*, 2013, **31**, 559.
- 35 F. Sun, C. Yan, Z. Wang, C. Guo and S. Huang, *Int. J. Hydrogen Energy*, 2015, **40**, 15985.
- 36 J. A. Farmer and C. T. Campbell, *Science*, 2010, **329**, 933.
- 37 L. Wang, S. Zhang and Y. Liu, *J. Rare Earths*, 2008, **26**, 66.
- 38 L. Wang, H. Liu, Y. Liu, Y. Chen and S. Yang, *J. Rare Earths*, 2013, **31**, 969.
- 39 B. Lu and K. Kawamoto, *Mater. Res. Bull.*, 2014, **53**, 70.
- 40 H. C. Wu, Y. C. Chang, J. H. Wu, J. H. Lin, I. K. Lin and C. S. Chen, *Catal. Sci. Technol.*, 2015, **5**, 4154.
- 41 A. A. Upadhye, I. Ro, X. Zeng, H. J. Kim, I. Tejedor, M. A. Anderson, J. A. Dumesic and G. W. Huber, *Catal. Sci. Technol.*, 2015, **5**, 2590.
- 42 J. A. Rodriguez, J. Evans, L. Feria, A. B. Vidal, P. Liu, K. Nakamura and F. Illas, *J. Catal.*, 2013, **307**, 162.
- 43 P. C. Zonetti, S. Letichevsky, A. B. Gaspar, E. F. Sousa-Aguiar and L. G. Appel, *Appl. Catal., A*, 2014, **475**, 48.
- 44 L. C. Wang, D. Widmann and R. J. Behm, *Catal. Sci. Technol.*, 2015, **5**, 925.
- 45 D. Tibiletti, A. Goguet, F. C. Meunier, J. P. Breen and R. Burch, *Chem. Commun.*, 2004, **40**, 1636.
- 46 F. C. Meunier, D. Tibiletti, A. Goguet, D. Reid and R. Burch, *Appl. Catal., A*, 2005, **289**, 104.
- 47 D. Tibiletti, A. Goguet, D. Reid, F. C. Meunier and R. Burch, *Catal. Today*, 2006, **113**, 94.
- 48 A. Goguet, F. C. Meunier, D. Tibiletti, J. P. Breen and R. Burch, *J. Phys. Chem. B*, 2004, **108**, 20240.
- 49 G. Jacobs and B. H. Davis, *Appl. Catal., A*, 2005, **284**, 31.
- 50 A. Goguet, S. O. Shekhtman, R. Burch, C. Hardacre, F. C. Meunier and G. S. Yablonsky, *J. Catal.*, 2006, **237**, 102.
- 51 L. C. Wang, M. T. Khazaneh, D. Widmann and R. J. Behm, *J. Catal.*, 2013, **302**, 20.
- 52 A. Goguet, F. Meunier, J. P. Breen, R. Burch, M. I. Petch and A. F. Ghenciu, *J. Catal.*, 2004, **226**, 382.
- 53 C. Li, S. Zhang, B. Zhang, D. Su, S. He, Y. Zhao, J. Liu, F. Wang, M. Wei, D. G. Evans and X. Duan, *J. Mater. Chem. A*, 2013, **1**, 2461.
- 54 P. J. Lunde and F. L. Kester, *Ind. Eng. Chem. Process Des. Dev.*, 1974, **13**, 27.
- 55 A. Beuls, C. Swalus, M. Jacquemin, G. Heyen, A. Karelovic and P. Ruiz, *Appl. Catal., B*, 2012, **113–114**, 2.
- 56 P. A. U. Aldana, F. Ocampo, K. Kobl, B. Louis, F. Thibault-Starzyk, M. Daturi, P. Bazin, S. Thomas and A. C. Roger, *Catal. Today*, 2013, **215**, 201.
- 57 S. Rahmani, M. Rezaei and F. Meshkani, *J. Ind. Eng. Chem.*, 2014, **20**, 1346.
- 58 J. Liu, C. Li, F. Wang, S. He, H. Chen, Y. Zhao, M. Wei, D. G. Evans and X. Duan, *Catal. Sci. Technol.*, 2013, **3**, 2627.
- 59 E. Jwa, S. B. Lee, H. W. Lee and Y. S. Mok, *Fuel Process. Technol.*, 2013, **108**, 89.
- 60 M. Cai, J. Wen, W. Chu, X. Cheng and Z. Li, *J. Nat. Gas Chem.*, 2011, **20**, 318.
- 61 G. Garbarino, D. Bellotti, P. Riani, L. Magistri and G. Busca, *Int. J. Hydrogen Energy*, 2015, **40**, 9171.

- 62 S. Tada, T. Shimizu, H. Kameyama, T. Haneda and R. Kikuchi, *Int. J. Hydrogen Energy*, 2012, **37**, 5527.
- 63 F. Ocampo, B. Louis and A. Roger, *Appl. Catal., A*, 2009, **369**, 90.
- 64 R. Razzaq, H. Zhu, L. Jiang, U. Muhammad, C. Li and S. Zhang, *Ind. Eng. Chem. Res.*, 2013, **52**, 2247.
- 65 S. Tada, O. J. Ochieng, R. Kikuchi, T. Haneda and H. Kameyama, *Int. J. Hydrogen Energy*, 2014, **39**, 10090.
- 66 Q. Pan, J. Peng, T. Sun, S. Wang and S. Wang, *Catal. Commun.*, 2014, **45**, 74.
- 67 C. Leitenburg, A. Trovarelli and J. Kašpar, *J. Catal.*, 1997, **166**, 98.
- 68 S. Sharma, Z. Hu, P. Zhang, E. W. McFarland and H. Metiu, *J. Catal.*, 2011, **278**, 297.
- 69 D. C. Upham, A. R. Derk, S. Sharma, H. Metiu and E. W. McFarland, *Catal. Sci. Technol.*, 2015, **5**, 1783.
- 70 F. Ocampo, B. Louis, L. Kiwi-Minsker and A. Roger, *Appl. Catal., A*, 2011, **392**, 36.
- 71 H. Zhu, R. Razzaq, C. Li, Y. Muhammad and S. Zhang, *AIChE J.*, 2013, **59**, 2567.
- 72 R. Razzaq, C. Li, N. Amin, S. Zhang and K. Suzuki, *Energy Fuels*, 2013, **27**, 6955.
- 73 H. Liu, X. Zou, X. Wang, X. Lu and W. Ding, *J. Nat. Gas Chem.*, 2012, **21**, 703.
- 74 J. Ma, N. N. Sun, X. L. Zhang, N. Zhao, F. K. Mao, W. Wei and Y. H. Sun, *Catal. Today*, 2009, **148**, 221.
- 75 N. Kumari, N. Sinha, M. A. Haider and S. Basu, *Electrochim. Acta*, 2015, **177**, 21.
- 76 J. Weigel, R. A. Koepfel, A. Baiker and A. Wokaun, *Langmuir*, 1996, **12**, 5319.
- 77 C. Schild, A. Wokaun and A. Baiker, *J. Mol. Catal.*, 1990, **63**, 243.
- 78 K. T. Jung and A. T. Bell, *J. Catal.*, 2001, **204**, 339.
- 79 D. L. Chiavassa, S. E. Collins, A. L. Bonivardi and M. A. Baltanas, *Chem. Eng. J.*, 2009, **150**, 204.
- 80 J. Liu, J. Shi, D. He, Q. Zhang, X. Wu, Y. Liang and Q. Zhu, *Appl. Catal., A*, 2001, **218**, 113.
- 81 J. Słoczyński, R. Grabowski, A. Kozłowska, P. Olszewski, J. Stoch, J. Skrzypek and M. Lachowska, *Appl. Catal., A*, 2004, **278**, 11.
- 82 J. Toyir, P. Piscina, J. Fierro and N. Homs, *Appl. Catal., B*, 2001, **34**, 255.
- 83 X. An, J. Li, Y. Zuo, Q. Zhang, D. Wang and J. Wang, *Catal. Lett.*, 2007, **118**, 264.
- 84 X. Liang, X. Dong, G. Lin and H. Zhang, *Appl. Catal., B*, 2009, **88**, 315.
- 85 L. Jia, J. Gao, W. Fang and Q. Li, *Catal. Commun.*, 2009, **10**, 2000.
- 86 X. Yang, S. Kattel, S. D. Senanayake, J. A. Boscoboinik, X. Nie, J. Graciani, J. A. Rodriguez, P. Liu, D. J. Stacchiola and J. G. Chen, *J. Am. Chem. Soc.*, 2015, **137**, 10104.
- 87 G. Bonura, F. Arena, G. Mezzatesta, C. Cannilla, L. Spadaro and F. Frusteri, *Catal. Today*, 2011, **171**, 251.
- 88 F. Arena, G. Mezzatesta, G. Zafarana, G. Trunfio, F. Frusteri and L. Spadaro, *J. Catal.*, 2013, **300**, 141.
- 89 Z. Cheng, Q. Wu, J. Li and Q. Zhu, *Catal. Today*, 1996, **30**, 147.
- 90 F. Wang, L. Xu, J. Zhang, Y. Zhao, H. Li, H. X. Li, K. Wu, G. Q. Xu and W. Chen, *Appl. Catal., B*, 2016, **180**, 511.
- 91 M. Fan, A. Z. Abdullah and S. Bhatia, *ChemCatChem*, 2009, **1**, 192.
- 92 A. C. Luntz and J. Harris, *Surf. Sci.*, 1991, **258**, 397.
- 93 F. Solymosi, *J. Mol. Catal.*, 1991, **65**, 337.
- 94 J. Segner, C. T. Campbell, G. Doyen and G. Ertl, *Surf. Sci.*, 1984, **138**, 505.
- 95 R. Wang, H. Xu, X. Liu, Q. Ge and W. Li, *Appl. Catal., A*, 2006, **305**, 204.
- 96 S. Zhang, S. Muratsugu, N. Ishiguro and M. Tada, *ACS Catal.*, 2013, **3**, 1855.
- 97 S. Wang and G. Q. Lu, *Appl. Catal., B*, 1998, **19**, 267.
- 98 H. Roh, H. S. Potdar and K. Jun, *Catal. Today*, 2004, **93–95**, 39.
- 99 V. M. Gonzalez-DelaCruz, J. P. Holgado, R. Pereñíguez and A. Caballero, *J. Catal.*, 2008, **257**, 307.
- 100 S. Damyanova, B. Pawelec, K. Arishtirova, M. V. M. Huerta and J. L. G. Fierro, *Appl. Catal., B*, 2009, **89**, 149.
- 101 D. C. Carvalho, H. S. A. Souza, J. M. Filho, A. C. Oliveira, A. Campos, É. R. C. Milet, F. F. Sousa, E. Padron-Hernandez and A. C. Oliveira, *Appl. Catal., A*, 2014, **473**, 132.
- 102 S. Corthals, J. V. Nederkassel, H. D. Winne, J. Geboers, P. Jacobs and B. Sels, *Appl. Catal., B*, 2011, **105**, 263.
- 103 J. Kim, D. Suh, T. Park and K. Kim, *Appl. Catal., A*, 2000, **197**, 191.
- 104 H. T. Liu, S. Q. Li, S. B. Zhang, J. M. Wang, G. J. Zhou, L. Chen and X. L. Wang, *Catal. Commun.*, 2008, **9**, 51.
- 105 V. R. Choudhary, A. M. Rajput and B. Prabhakar, *Catal. Lett.*, 1995, **32**, 391.
- 106 J. G. Zhang, H. Wang and A. K. Dalai, *J. Catal.*, 2007, **249**, 300.
- 107 K. Nagaoka, K. Takanabe and K. Aika, *Catal. Commun.*, 2001, **2**, 255.
- 108 I. G. O. Črnivec, P. Djinović, B. Erjavec and A. Pintar, *Chem. Eng. J.*, 2012, **207–208**, 299.
- 109 P. Djinović, I. G. O. Črnivec, B. Erjavec and A. Pintar, *Appl. Catal., B*, 2012, **125**, 259.
- 110 M. S. Aw, G. Dražić, P. Djinović and A. Pintar, *Catal. Sci. Technol.*, DOI: 10.1039/c5cy02082d.
- 111 P. Djinović, I. G. O. Črnivec and A. Pintar, *Catal. Today*, 2015, **253**, 155.
- 112 M. S. Aw, I. G. O. Črnivec, P. Djinović and A. Pintar, *Int. J. Hydrogen Energy*, 2014, **39**, 12636.